Title

Force-dependent trans-endocytosis by breast cancer cells depletes costimulatory receptor CD80 and attenuates T cell activation.

Authors

Park, Seungman

Shi, Yu

Kim, Byoung

et al.

Publication Date

2020-10-01

DOI

10.1016/j.bios.2020.112389

Peer reviewed

HHS Public Access

Author manuscript

Biosens Bioelectron. Author manuscript; available in PMC 2021 March 31.

Published in final edited form as:

Biosens Bioelectron. 2020 October 01; 165: 112389. doi:10.1016/j.bios.2020.112389.

Force-Dependent Trans-endocytosis by Breast Cancer Cells Depletes Costimulatory Receptor CD80 and Attenuates T Cell Activation

Seungman Park[1,8,9], **Yu Shi**[2], **Byoung Choul Kim**[3,4,5,6], **Myung Hyun Jo**[3], **Leilani O. Cruz**[7], **Zheming Gou**[1], **Taekjip Ha**[3,4,5], **Li-Fan Lu**[7], **Daniel H. Reich**[2], **Yun Chen**[1,8,9,*]

[1]Department of Mechanical Engineering, Johns Hopkins University, MD 21218, USA

[2]Department of Physics & Astronomy, Johns Hopkins University, MD 21218, USA

[3]Department of Biophysics and Biophysical Chemistry, Johns Hopkins School of Medicine, Baltimore, MD 21205, USA

[4]Department of Biomedical Engineering, Johns Hopkins University, Baltimore, MD 21218, USA

[5]Howard Hughes Medical Institute, Baltimore, MD 21205, USA

[6]Division of Nano-Bioengineering, Incheon National University, Incheon 22012, South Korea

[7]Division of Biological Science, University of California, San Diego, CA 92093, USA

[8]Center for Cell Dynamics, Johns Hopkins University, MD 21218, USA

[9]Institute for NanoBioTechnology, Johns Hopkins University, MD 21218, USA

Abstract

In this study, we investigated the biophysical interaction between cytotoxic T-lymphocyte-associated protein 4 (CTLA-4) and CD80. CTLA-4 is a key molecule in immunosuppression, and CD80 is a costimulatory receptor promoting T cell activation. We observed that after cell-cell contact was established between breast cancer cells and antigen presenting cells (APCs), CTLA-4 expressed on the breast cancer cells bind to CD80 expressed on the APCs, and underwent trans-endocytosis to deplete CD80. Force measurement and live cell imaging revealed that upon binding to CD80, forces generated by breast cancer cells and transmitted via CTLA-4 were sufficiently strong to displace CD80 from the surface of APCs to be internalized by breast cancer cells. We further demonstrated that because of the force-dependent trans-endocytosis of CD80, the capacity of APCs to activate T cells was significantly attenuated. Furthermore, inhibiting force generation in cancer cells would increase the T cell activating capacity of APCs. Our results provide a possible mechanism behind the immunosuppression commonly seen in breast cancer patients, and may lead to a new strategy to restore anti-tumor immunity by inhibiting pathways of force-generation.

[*]Corresponding Author: Yun Chen, Department of Mechanical Engineering, Johns Hopkins University, yun.chen@jhu.edu, Phone: +1-410-516-5194.

Author Contributions

Y.C. and L.-F.L conceived the study. S.P., Y.S., B.C.K., T.H., L.-F.L, D.H.R., and Y.C. designed the experiments. S.P., Y.S., B.C.K., M.H., L.O.C., Z.G., and Y.C. performed the experiments and data analysis. S.P. and Y.C. wrote the manuscript.

Introduction

Cytotoxic T-lymphocyte-associated protein 4 (CTLA-4), which is abundantly expressed in regulatory T (T_{reg}) cells (Hou et al., 2015), regulates immunity negatively (Bachmann et al., 1999; Bour-Jordan et al., 2011; Hou et al., 2015; Rudd, 2008; Wing et al., 2011). Recently, it was reported that CTLA-4 can be detected in many types of cancer cells (Pistillo et al., 2003). Coincidentally, immunosuppression is common among cancer patients (Sharma et al., 2017). The mechanisms by which cancer cells suppress immunity are yet to be fully elucidated and are likely to involve many pathways, depending on the physiological context. One of the possible pathways is through CTLA-4, in a similar fashion to how T_{reg} cells negatively modulate T cell activation. It has been reported that the T_{reg} cells deplete the costimulatory molecules CD80 and CD86 on antigen presenting cells (APCs) by trans-endocytosis (Qureshi et al., 2011; Walker and Sansom, 2011), and attenuate the T cell activation capacity of the APCs. Trans-endocytosis requires adequate force (Sakurai et al., 2014) for the engaged CTLA-4 to remove the target molecule from the surface of the APC and to internalize it (Walker, 2017). Given that many cancer cells are known to generate higher force via actomyosin contractility than their normal counterparts (Indra et al., 2011; Li et al., 2017; Przybyla et al., 2017), it is possible that cancer cells exploit force-dependent trans-endocytosis to deplete CD80 and suppress T cell activation.

In this work, we examined this possibility by measuring the force generated by breast cancer and normal cells, and transmitted through CTLA-4 when bound to CD80. We found that cancer cells transmitted higher force via CTLA-4 at the single-molecule and the cellular levels. Incubating breast cancer cells with CD80-expressing cells, we also found that the trans-endocytosis of CD80 by cancer cells is associated with attenuated T cell activation capacity of the CD80-expressing cells. Furthermore, we were able to restore the T cell activation capacity of the CD80-expressing cells if force generation was inhibited in cancer cells prior to the co-incubation. Our results suggest that force-dependent trans-endocytosis of costimulatory ligands on APCs is a possible mechanism of immunosuppression observed in cancer patients. We also demonstrated that targeting the force-generating pathways involved in trans-endocytosis can boost T cell activation. Our findings may inspire a new category of immunotherapy against cancer in patients.

Results

CTLA-4 is expressed on both normal and cancerous mammary epithelial cells

CTLA-4 is abundantly expressed in T_{reg} cells. Recently, CTLA-4 expression has also been observed in various cancer cells of breast carcinoma, melanoma, neuroblastoma, rhabdomyosarcoma and osteosarcoma, and neoplastic lymphoid and myeloid cells (Contardi et al., 2005a; Mao et al., 2010; Yu et al., 2015). In addition, CTLA-4 is also detected in normal cells other than T cells, such as peripheral blood mononuclear cells, B cells, $CD34^+$ stem cells, and granulocytes (Pistillo et al., 2003). We further examined whether CTLA-4 is also expressed in normal mammary epithelial cells of both murine and human origin, in addition to breast cancer cells. We performed immunofluorescence using anti-CTLA-4 in MCF10A (human) and EpH4-EV (mouse) cells, both of which are considered to be normal cells. The results were compared against those obtained in human and mouse breast cancer

cell lines, MDA-MB-231 and EO771, respectively (Figure 1a). We found that CTLA-4 can be detected in both normal and cancer cells, with MDA-MB-231 and EO771 cells expressing CTLA-4 at 40% and 30% higher than their normal counterparts, respectively (Figure 1b).

The tension in the bond between CTLA-4 and CD80 is higher in cancer cells

CD80 has been observed to be trans-endocytosed by cells expressing CTLA-4 (Ovcinnikovs et al., 2019; Qureshi et al., 2011). It has also been suggested that the trans-endocytosis and subsequent depletion of CD80, a costimulatory surface molecule involved in initiating T cell activation expressed on antigen presenting cells (APCs), is one of the mechanisms to achieve CTLA-4-dependent immunosuppression (Walker and Sansom, 2011). Consequentially, CD80-depleted APCs are no longer effective in activating T cells. Given that immunosuppression is common among breast cancer patients, it is possible that cancer cells expressing CTLA-4 also exploit trans-endocytosis to achieve CD80 depletion. Trans-endocytosis requires high forces (Egea and Klein, 2007; Malinova and Huveneers, 2018; Nichols et al., 2007), so that molecules immobilized on the surface of substrates or another cell could be torn away and internalized. The corollary of our hypothesis is that normal cells, while expressing a certain degree of CTLA-4, do not generate high enough forces to enable CD80 depletion by trans-endocytosis, allowing APCs to retain effective T cell activating capacity.

If higher forces are generated by the cancer cells, higher tension in the bond between CTLA-4 and CD80 will be detected. To test our hypothesis, we quantified the tension between CD80 and CTLA-4 using a double-strand DNA-based tension gauge tether (TGT) (Wang and Ha, 2013) in normal and cancer cells. A DNA strand of the TGT was immobilized on the substrate surface through biotin-neutravidin interaction and the complementary strand was conjugated with CD80 and a fluorophore, Cy3 (Figure 1c). The substrate surface was also coated with fibronectin to facilitate cell-substrate adhesion. Initially, the fluorescence emitted from Cy3 resulted in a bright background. When the pulling force transmitted from the cells via CTLA-4 exceeded the forces required to melt the duplex DNA, in this case, 12 pN, the DNA strand conjugated with CD80 and Cy3 was separated from the immobilized strand (Figures 1c and 1d), resulting in a loss-of-fluorescent signal event, or a “rupture event”, in the Cy3 fluorescence channel (Figure 1e). The dark pixels in the field of view thereby signified the events in which cells generated forces higher than 12 pN per CTLA-4 molecule. We observed that MDA-MB-231 cells exhibited 2.9-fold higher amounts of rupture events per unit area compared to MCF10A cells, and EO771 cells exhibited 1.3-fold higher amounts compared to EpH4-Ev cells (Figure 1f). The results suggest that the force required to rupture the bond between the CTLA-4 and CD80 is higher than 12 pN, and that breast cancer cells have more CTLA-4 molecules capable of transmitting forces exceeding 12 pN than normal cells. To further evaluate whether the observation that cancer cells have more CTLA-4 molecules capable of transmitting forces exceeding 12 pN leads to trans-endocytosis of CD80 in cancer cells in a force-dependent manner, we proceeded to compare forces generated by normal and cancer cells at the cellular level.

Forces transmitted via CTLA-4 are higher in cancer cells

Given that cancer cells express more CTLA-4 molecules (Figure 1b), and have significantly more CTLA-4 molecules capable of transmitting forces than 12 pN (Figure 1f), we postulated that at the cellular level, cancer cells exert higher forces to facilitate the trans-endocytosis of CD80. To test this, we measure the forces transmitted onto micrometer-sized objects coated with CD80, at either the dorsal or ventral side of the cell. We first seek to measure the forces at the dorsal side the cell. Microfluidic devices, a powerful tool for cell analysis and sorting techniques (Chen et al., 2016; Guo et al., 2015; Park et al., 2018; Shi et al., 2015; Xue et al., 2016), are ideal to probe the mechanical behaviors at the dorsal side of the cell in a high-throughput manner. To measure the forces transmitted through CTLA-4 distributed at the dorsal side of the cell, we used a microfluidic device previously developed by our group (Figure 2a) (Park et al., 2019), where a constant hydrodynamic force of approximately 14 pN was applied to cells cultured in a flow chamber and decorated with CD80-conjugated particles. By tracking the displacement of the particles moving against the flow direction, the forces generated by the cells to overcome the hydrodynamic forces could be calculated (Figures 2b and 2c). About 16% of the total particles bound to MCF10A cells moved against the flow, and 11% of the total particles bound to MDA-MB-231 moved against the flow (Figure 2d). The force generated by MDA-MB-231 cells to displace the particles was approximately 1.5-fold higher than MCF10A cells (Figure 2e). Next, we measured the forces at the ventral side of the cell using micropillar arrays (Fu et al., 2010) (Figure 2f). The micropillars were coated with fibronectin and CD80. The fibronectin ensured that cells adhered to the substrate properly. As a control, we also measured the forces generated by cells on micropillars coated with fibronectin only. We observed significantly higher forces generated on the micropillars coated with CD80 and fibronectin, than for the fibronectin-only group (Figures 2g and 2h). Notably, both MCF10A and MDA-MB231 cells generated higher forces when seeded on the micropillars coated with CD80 and fibronectin than fibronectin only. This suggests that cells transmit forces via both integrin and CTLA-4, which are the binding partners for fibronectin and CD80, respectively. A similar trend was observed in EO771 cells (Figure supplement 1). Furthermore, we observed that when on micropillars coated with CD80 and fibronectin, MDA-MB-231 cells generated 1.8-fold higher forces than MCF10A cells (Figures 2g and 2h).

CD80 depletion is force-dependent and results in suppressed T cell activation

Having observed that CTLA-4 molecules on cancer cells transmit higher forces, we next examined whether cancer cells can suppress T cell activation, like T_{reg} cells, via trans-endocytosis of CD80 (Walker and Sansom, 2011), which is a force-dependent process (Figure 3a). First, we co-incubated MDA-MB-231 or MCF10A cells with T cell stimulator (TCS-CD80) cells derived from murine thymoma cells Bw5417. The TCS-CD80 cells express membrane-bound CD80 and membrane-bound anti-human CD3 antibody fragments (Jutz et al., 2016; Leitner et al., 2010), and are capable of T cell activation. This is because CD80 binds to CD28 (Boulougouris et al., 1998) on the T cell surface, and anti-CD3 fragment binds to CD3 (Tsoukas et al., 1985) on the T cell surface; CD28, and CD3, once bound to CD80 and anti-CD3, respectively, trigger signaling cascades collectively leading to T cell activation. During the co-incubation, the MDA-MB-231 cells dynamically interacted with the TCS-CD80 cells. The two cell types were observed to be in constant contact with

each other through their ruffling plasma membranes (Video Supplements 1 and 2). After 12 hours of co-incubation, immunofluorescence targeting CD80 and CTLA-4 was performed (Figure 3b). We detected CD80 in MDA-MB-231 but not in MCF10A cells. Furthermore, upon visual inspection, the fluorescence intensity of anti-CD80 staining was dimmer on TCS-CD80 co-incubated with MDA-MB231 cells, indicating MDA-MB-231 cells internalized CD80 on the surface of the TCS-CD80 cells by trans-endocytosis.

To evaluate whether the depletion of CD80 on the surface of TCS-CD80 cells affected their capacity for T cell activation, the TCS-CD80 cells co-incubated either with MDA-MB-231 or MCF10A cells were isolated from the co-incubation, and then mixed with T cell activation reporter cells (TRCs) (Figure 3c). The TRCs are derived from Jurkat T cells with the DNA sequences of NF-κB-binding-motif-CFP and NFAT-binding-motif-eGFP introduced into the genome. TRCs transfected with NF-κB-binding-motif-CFP and NFAT-binding-motif-eGFP will express CFP when NF-κB is active, and express eGFP when NFAT is active. Both NF-κB and NFAT are required for T cell activation (Jutz et al., 2016). Therefore, NF-κB-CFP and NFAT-eGFP serve as reporters of T cell activation in the TRCs.

After TRCs were co-incubated for 12 hours with the TCS-CD80 cells, which had been previously in contact with MDA-MB-231 or MCF10A cells, we assessed the NF-κB and NFAT activities by quantifying the fluorescence intensity of CFP and eGFP, respectively. 19.4% of the TRCs exhibited NF-κB and NFAT activation when co-incubated with MCF10A cells, while only 10.7% of TRCs exhibited the same level of activation when co-incubated with MDA-MB-231 cells (Figures 3d and 3e). None of the TRCs exhibited NF-κB and NFAT activation when cultured alone. Taken together, MDA-MB-231 cells generate higher forces, thereby depleting CD80 by trans-endocytosis and suppressing the T cell activation capacity of TCS-CD80 cells.

To establish further the causality between force, CD80 trans-endocytosis and immunosuppression, we treated MDA-MB-231 cells with blebbistatin, an inhibitor of the force-generating molecule myosin II (Kovács et al., 2004). Trans-endocytosis of CD80 was suppressed when TCS-CD80 cells were co-incubated with blebbistatin-treated MDA-MB-231 cells (Figure 3b). Moreover, 73.6% of TRCs exhibited NF-κB and NFAT activation when co-incubated with blebbistatin-treated MDA-MB-231 cells (Figure 3f), about 7-fold higher than with the control MDA-MB-231 cells (Figure 3e). These results confirmed force-dependent trans-endocytosis of CD80 is involved in the suppression of T cell activation. Similarly, when MCF10A cells were treated with blebbistatin, 63.2% of the TRCs exhibit NF-κB and NFAT activation (Figure supplement 2). The result that myosin inhibition in MCF10A cells further increased T cell activation suggests that when cells express CTLA-4, as MCF10A cells do (Figure 1a), they are capable of immunosuppression via a variety of mechanisms not limited to trans-endocytosis. In the case of MCF10A cells, though trans-endocytosis is not required in the CTLA-4-mediated immunosuppression (Figure 3b), baseline myosin activity is required.

Discussion

In this study, we observed that while CTLA-4 is expressed in both normal and breast cancer cells. While both normal and cancer cells generate forces detectable at the molecular and cellular levels, only cancer cells can transmit high forces to facilitate trans-endocytosis of CD80 when it is bound to CTLA-4. We demonstrated that trans-endocytosis of CD80 is a force-dependent process that can attenuate the capacity of T cell activation (Figure 4). Inhibition of force generation in cancer cells can rescue the suppressive effect on T cell activation by cancer cells. Our finding provides a possible explanation of how cancer cells evade immunity by suppressing T cell activation. Interestingly, myosin II inhibition in MDA-MB-231 cells resulted in a 7-fold increase in T cell activation by TCS-CD80 cells (Figure 3f), exceeding even the extent of T cell activation when TCS-CD80 cells were co-incubated with MCF10A cells (Figure 3d), which transmitted lower forces via CTLA-4. Combined with the observation that myosin II inhibition in MCF10A cells also enhanced T cell activation, our results imply that the existence of a different myosin-dependent mechanism other than trans-endocytosis to suppress the capacity of T cell activation in TCS-CD80 cells. Indeed, multiple mechanisms not involving trans-endocytosis have been reported or proposed (Alegre et al., 2001; Bour-Jordan et al., 2011; Walker and Sansom, 2011). It is plausible that while the myosin activity in MCF10A cells is not adequate for trans-endocytosis of CD80, it is sufficient to sustain other pathways leading to CTLA-4-mediated immunosuppression. In other words, suppression of T cell activation was possibly resulting from multiple myosin-dependent pathways in MDA-MB-231 cells, including trans-endocytosis of CD80, whereas suppression by MCF10A was from pathways excluding trans-endocytosis of CD80. Therefore, less T cell activation was observed in TPRs associated with MDA-MB-231 cells (Figures 3d and 3e). As blebbistatin inactivated trans-endocytosis of CD80, along with other myosin-dependent pathways, the extents of T cell activation became comparable in TPRs associated with blebbistatin-treated MDA-MB-231 and MCF10A cells (Figures 3f, supplement 2).

It should be noted that the detection of CTLA-4 on MCF10A cells in this study adds to a growing list of normal cells expressing CTLA-4, in addition to T_{reg} cells (Kaufman et al., 1999; Pico de Coaña et al., 2014). To maintain homeostasis, CTLA-4 expressed in normal cells attenuates T cell activation, so that undesired autoimmunity and excessive inflammation is prevented (Choi et al., 2006; Thompson and Allison, 1997; Vijayakrishnan et al., 2004). Compared to MDA-MB-231 cells, we observed a relatively modest attenuation by MCF10A cells, which could be within the healthy range of immune regulation. On the other hand, cancer cells possibly exploit their elevated actomyosin contractility to achieve trans-endocytosis of CD80, suppressing T cell activation even when such activation is needed.

In our previous study, we observed that the force magnitude breaking the bond between CTLA-4 and CD80 is at least two-fold higher than the magnitude of the endocytic force (Park et al., 2019). This explains why that CD80 was depleted from the cell membrane of the APC through CTLA-4-mediated trans-endocytosis (Figure 3b), rather than remaining at the surface of the APC as the result of bond-breaking between CD80 and CTLA-4.

In this study, we observed force-dependent CTLA-4-mediated trans-endocytosis in two breast cancer cell lines, MDA-MB-231 and EO771. It is likely that CTLA4-mediated trans-endocytosis of CD80 also occurs in other types of cancer, in addition to the breast cancer cell lines MDA-MB-231 and EO771 tested in this study. We postulated that cancer cells expressing CTLA-4 are capable of conducting trans-endocytosis of CD80 which requires high force generation, based on two observations previously reported by other groups: (1) CTLA-4 is abundantly expressed in many types of cancer cells (Contardi et al., 2005b; Laurent et al., 2013; Mao et al., 2010; Paulsen et al., 2017; Pistillo, 2003; Yu et al., 2015); and (2) Many types of cancer cells are reported to generate higher forces through myosin-mediated pathways (Indra et al., 2011; Koch et al., 2012; Kraning-Rush et al., 2012; Northcott et al., 2018). Indeed, by immunofluorescence, we have observed that murine early-stage breast cancer cells 67NR, metastatic breast cancer cells EO771, metastatic breast cancer cells 4T1, and sarcoma cells 9609 express higher level of CTLA-4 compared to the normal epithelial cells EpH4-EV (Fig. S3). Furthermore, in our previous study, we found that the murine early-stage breast cancer cell line 67NR, with abundant CTLA-4 expression, also exerts higher forces relative to its normal counterpart EpH4-EV (Jung et al., 2020). Therefore, many types of cancer cells might use CTLA-4-mediated trans-endocytosis as a common mechanism to evade immunity. It merits further investigation to verify whether inhibiting force generation can be a common approach to boost anti-cancer immunity, in addition to breast cancer.

Trans-endocytosis of surface molecules expressed on another cell has also been observed in Notch-ligand (Andersson, 2012; Meloty-Kapella et al., 2012), the gap junction protein connexin-43 (Falk et al., 2014), and the adherens junction protein VE-cadherin (Sakurai et al., 2014), initiating signal transduction, protein turnover, and cellular component exchange, respectively. Our results indicate trans-endocytosis might also be exploited by cancer cells to evade immunity. Targeting molecules involved in trans-endocytosis by cancer cells might effectively promote immunity in cancer patients.

Materials and Methods

Cell culture

Human breast carcinoma cells MDA-MB-231 (ATCC) and mouse mammary epithelial cells EpH4-EV (ATCC) were maintained in DMEM (#11995073, ThermoFisher). The immortalized mouse breast carcinoma cell line EO771 cells (ATCC) were maintained in RPMI 1640 (#11875093, ThermoFisher). The DMEM and RPMI 1640 culture media were supplemented with 10% fetal bovine serum (#26140079, ThermoFisher) and 100 U/mL penicillin and 100 μg/mL streptomycin (1% P/S) (#15140122, ThermoFisher). The immortalized mammary epithelial cell line MCF10A cells (ATCC) were maintained in MEBM (#CC-3151, Lonza). The MEBM medium was supplemented with hEGF (0.1% v/v), insulin (0.1% v/v), hydrocortinsone (0.1% v/v), BPE (0.4% v/v), and cholera toxin (100 ng/ml) using the supplement kit (#CC-4136, Lonza). TRCs and TCS-CD80 cells were a generous gift from Dr. Peter Steinberger (Jutz et al., 2016). TRC and TCS-CD80 cells were maintained in RPMI 1640 supplemented with 10% fetal bovine serum.

Immunofluorescence and image analysis

For CTLA-4, cells were fixed with 4% paraformaldehyde (#19943, Affymetrix) and permeabilized by 0.1% Triton X-100. The fixed cells were stained with human (#349907, BioLegend) or mouse (#106204, BioLegend) anti-CTLA4 antibody. For CD3 and CD80, human anti-CD3 antibody (#317302, BioLegend) and anti-CD80 antibody (#2D10, BioLegend) were used to stain the fixed cells, respectively. Images were acquired using a confocal microscope (Leica SP8).

The fluorescence intensity of cells stained with fluorescently labeled antibody or expressing fluorescent proteins was determined using FIJI-ImageJ (NIH) of each cell were calculated. The intensity value was corrected by subtracting the mean of background intensity.

Myosin II inhibition

MDA-MB-231 cells were treated with 20 μM blebbistatin (#B0560, Sigma-Aldrich) for 2 hours prior to the co-incubation with TCS-CD80 cells. The medium for the co-incubation also contained 20 μM blebbistatin.

Tension gauge tether (TGT) measurement

TGTs with the tension tolerance of 12 pN were synthesized by combining two ssDNAs (Integrated DNA Technologies, Inc.): ssDNA conjugated with ProG (ab49807, Abcam. Recombinant ProG with 6-His tag for purification) and Cy3, and ssDNA conjugated with biotin. The sequences for the two ssDNA are shown as follows:

- 5-/5Cy3/GGC CCG CAG CGA CCA CCC/3ThioMC3-D/ −3
- 5-/5Biosg/-GGG TGG TCG CTG CGG GCC3

After hybridizing ProG-ssDNA with complementary ssDNA-biotin, ProG-TGT composed of two ssDNAs is mixed with CD80-Fc (#555404, BioLegend) at 1:1 molar ratio (i.e., CD80-Fc/ProG-TGT) (Wang et al., 2016). Glass-bottom dishes were coated with biotinylated bovine serum albumin (BSA) at 1 mg/ml (#29130, ThermoFisher) for 1 hour. After washing three times using PBS, neutravidin (NA, 200 μg/ml, #31000, ThermoFisher) was added to the dish to immobilize TGT through a biotin-NA bond on the BSA glass surface. Finally, 10 μL of CD80-Fc/ProG-TGT (0.15 μM) was added onto the NA-coated surface, and the surface was incubated at 4 °C for 30 minutes and washed three times using PBS.

10^4 cells were seeded on the glass-bottom dish and incubated for 30 minutes at 37 °C. Then the cells were fixed using 4 % paraformaldehyde by incubating at room temperature for 10 minutes. After washing three times using PBS, the samples were stored in 4 °C until imaging.

For imaging, fluorescence, reflectance, and transmission images were taken using the confocal microscope (Leica SP8) and 40x water immersion objective lens. To quantify intensity loss due to TGT rupture, the corrected intensity was calculated by subtracting average background intensity from average intensity within cells.

Prediction of tension tolerance (rupture force) of TGT

The rupture force was estimated by a ladder model for DNA hybrids as reported (de Gennes, 2001; Wang and Ha, 2013):

$$F = 2f_c\left[\chi^{-1}\tanh\left(\chi\frac{L}{2}\right)+1\right] \quad (1)$$

where F, 2fc and L represent the total rupture force, the rupture force for one single band. DNA base pair number. χ-1 can be obstained by calculating the value of (Q/2R)0.5, where Q represents the spring constant of the backbone, and R represents the spring constant of the bond between base pairs. More details for the geometry and parameters used in TGT calculation are presented in (Wang and Ha, 2013).

Dorsal force measurement

50,000 cells were seeded in a microfluidic channel (#80666, μ-Slide VI 0.1, Ibidi). and incubated at 5% CO_2 and 37 °C for 24 hours. Micron-sized particles (#10003D, 2.8-μm Dynabeads, ThermoFischer) decorated with CD80-Fc (#555404, Biolegend) were flowed into the microfluidic channel to bind to the cells. A 14-pN hydrodynamic force was generated by flowing the medium through the microfluidic channel with at appropriate flow rate using a syringe pump (#NE-1002X, Pump System Inc.). The cell-bound particles were then imaged at 10-second interval for 5 minutes at 10x magnification. The particle displacement and velocity were quantified using TrackMate, a plugin function of FIJI-ImageJ. The forces generated by cells were estimated by summing the applied hydrodynamic force and interfacial drag (Park et al., 2019).

Ventral force measurement

Micropillar arrays were fabricated in polydimethylsiloxane (PDMS) via replica molding on 22 mm cover glasses (Tan et al., 2003). The micropillars were 1.8 μm in diameter and 9.1 μm in height with 4 μm center-to-center spacing in a hexagonal pattern. For small deflections in response to lateral force applied to their tips, these micropillars yield an effective spring constant of 5.5 nN/μm (Fu et al., 2010). The micropillar arrays were first dried using a critical point dryer (Tousimis) in liquid CO_2 to avoid surface tension during evaporation causing collapse of the micropillars and were then treated in UV Ozone for 7 minutes for surface activation. 100 μl of 5 μg/ml fibronectin or 50 μl of 5 μg/ml fibronectin mixed with 50 μl of 15 μg/ml of CD-80 were added on top of a flat PDMS stamp (mixed 1:30 with curing agent) for one hour to allow the solution to be fully absorbed. The stamps were then washed with DI water and dried with Nitrogen gas, stamped on top of the arrays for a few seconds to coat the micropillars' tips, and peeled off in 100% ethanol. The arrays were then washed with 70% ethanol and DI water consecutively, and then treated with 0.2% W/V Pluronics F-127 for 30 minutes to block cell adhesion on the micropillars' unfunctionalized sides and the other surfaces of the arrays.

Cells were seeded onto the arrays at a density of 10^4 cells per 30-mm culture dish and cultured for 12 hours before imaging. Cells were imaged with an inverted microscope (Nikon TE-2000E) using a 40x, NA = 0.6, extra-long working distance air objective (Nikon

Plan Fluor). The positions of the micropillars were extracted using a centroid-based particle tracking algorithm (Crocker and Grier, 1996) in Igor Pro (Wavemetrics) (Shi et al., 2019). Static forces were calculated based on the displacement of the tips from their undeflected positions, which were determined via interpolation of the hexagonal grid based on the positions of posts not attached to cells (Sniadecki et al., 2008, 2007). The magnitude sum of static force from all micropillars underneath the cells was reported as the total force of each cell. To compare the force generation across different cell types, which have different average areas, as well as different integrin and CTLA4 expression, the forces generated are normalized in the following way. The force magnitude when the micropillars were coated only with fibronectin was used as the baseline for the cell type being measured. After the force magnitude was measured on the micropillars coated with fibronectin and CD80 in the same cell type, the fold increase in forces compared to the baseline magnitude was then determined. Such fold increases of MDA-MB-231 and MCF10A were compared to assess how much additional force was generated because of the bond formation between CTLA-4 and CD80.

T cell activation assay

10^5 cells of MDA-MB-231 or MCF10A were seeded onto the glass bottom dishes (#D29-20-1-N, Cellvis). TCS-CD80 cells (5×10^3 cells/well) were added incubated at 37 °C and 5% CO_2 for 24 hours. TCS-CD80 cells were separated from the co-incubation with by aspiration and mixed with TRCs (5×10^4/well) for 4 hours. The cells were fixed with 4% paraformaldehyde and stained with anti-human CD3 (#317302, BioLegend). Images were acquired using the Leica SP8 confocal microscope. TRCs were first identified in the acquired image by high fluorescence intensity of the anti-CD3. The NF-κB and NFAT activities were determined in the $CD3^+$ cells by the fluorescence intensity of CFP and GFP, respectively. ImageJ was used for the quantification of fluorescence intensity.

Statistical analysis

Each experimental group was repeated at least three times ($n \geq 3$). The results were analyzed using a one-factor ANOVA for statistical analysis, and the differences were considered statistically significant when p is less than 0.05. Results are presented as the mean ± standard deviation.

Supplementary Material

Refer to Web version on PubMed Central for supplementary material.

References

Alegre M-L, Frauwirth K. a, Thompson CB, 2001. T-cell regulation by CD28 and CTLA-4. Nat. Rev. Immunol 1, 220–228. 10.1038/35105024 [PubMed: 11905831]

Andersson ER, 2012. The role of endocytosis in activating and regulating signal transduction. Cell. Mol. Life Sci 69, 1755–1771. 10.1007/s00018-011-0877-1 [PubMed: 22113372]

Bachmann MF, Köhler G, Ecabert B, Mak TW, Kopf M, 1999. Cutting edge: lymphoproliferative disease in the absence of CTLA-4 is not T cell autonomous. J. Immunol 163, 1128–31. [PubMed: 10415006]

Boulougouris G, McLeod JD, Patel YI, Ellwood CN, Walker LS, Sansom DM, 1998. Positive and negative regulation of human T cell activation mediated by the CTLA-4/CD28 ligand CD80. J. Immunol 161, 3919–24. [PubMed: 9780158]

Bour-Jordan H, Esensten JH, Martinez-Llordella M, Penaranda C, Stumpf M, Bluestone JA, 2011. Intrinsic and extrinsic control of peripheral T-cell tolerance by costimulatory molecules of the CD28/B7 family. Immunol. Rev 10.1111/j.1600-065X.2011.01011.x

Chen Y, Guo J, Muhammad H, Kang Y, Ary SK, 2016. CMOS-compatible silicon-nanowire-based Coulter counter for cell enumeration. IEEE Trans. Biomed. Eng 10.1109/TBME.2015.2456190

Choi J-M, Ahn M-H, Chae W-J, Jung Y-G, Park J-C, Song H-M, Kim Y-E, Shin J-A, Park C-S, Park J-W, Park T-K, Lee J-H, Seo B-F, Kim K-D, Kim E-S, Lee D-H, Lee Seung-Kyou, Lee Sang-Kyou, 2006. Intranasal delivery of the cytoplasmic domain of CTLA-4 using a novel protein transduction domain prevents allergic inflammation. Nat. Med 12, 574–579. 10.1038/nm1385 [PubMed: 16604087]

Contardi E, Palmisano GL, Tazzari PL, Martelli AM, Falà F, Fabbi M, Kato T, Lucarelli E, Donati D, Polito L, Bolognesi A, Ricci F, Salvi S, Gargaglione V, Mantero S, Alberghini M, Ferrara GB, Pistillo MP, 2005a. CTLA-4 is constitutively expressed on tumor cells and can trigger apoptosis upon ligand interaction. Int. J. Cancer 117, 538–550. 10.1002/ijc.21155 [PubMed: 15912538]

Contardi E, Palmisano GL, Tazzari PL, Martelli AM, Falà F, Fabbi M, Kato T, Lucarelli E, Donati D, Polito L, Bolognesi A, Ricci F, Salvi S, Gargaglione V, Mantero S, Alberghini M, Ferrara GB, Pistillo MP, 2005b. CTLA-4 is constitutively expressed on tumor cells and can trigger apoptosis upon ligand interaction. Int. J. Cancer 117, 538–50. 10.1002/ijc.21155 [PubMed: 15912538]

Crocker JC, Grier DG, 1996. Methods of digital video microscopy for colloidal studies. J. Colloid Interface Sci 10.1006/jcis.1996.0217

de Gennes P-G, 2001. Maximum pull out force on DNA hybrids. Comptes Rendus l'Académie des Sci. - Ser. IV - Phys 2, 1505–1508. 10.1016/S1296-2147(01)01287-2

Egea J, Klein R, 2007. Bidirectional Eph-ephrin signaling during axon guidance. Trends Cell Biol. 10.1016/j.tcb.2007.03.004

Falk MM, Kells RM, Berthoud VM, 2014. Degradation of connexins and gap junctions. FEBS Lett. 588, 1221–1229. 10.1016/j.febslet.2014.01.031 [PubMed: 24486527]

Fu J, Wang YK, Yang MT, Desai RA, Yu X, Liu Z, Chen CS, 2010. Mechanical regulation of cell function with geometrically modulated elastomeric substrates. Nat. Methods 7, 733–736. 10.1038/nmeth.1487 [PubMed: 20676108]

Guo J, Chen L, Huang X, Li CM, Ai Y, Kang Y, 2015. Dual characterization of biological cells by optofluidic microscope and resistive pulse sensor. Electrophoresis. 10.1002/elps.201400268

Hou TZ, Qureshi OS, Wang CJ, Baker J, Young SP, Walker LSK, Sansom DM, 2015. A Transendocytosis Model of CTLA-4 Function Predicts Its Suppressive Behavior on Regulatory T Cells. J. Immunol 194, 2148–2159. 10.4049/jimmunol.1401876 [PubMed: 25632005]

Indra I, Undyala V, Kandow C, Thirumurthi U, Dembo M, Beningo KA, 2011. An in vitro correlation of mechanical forces and metastatic capacity. Phys. Biol 8, 015015. 10.1088/1478-3975/8/1/015015 [PubMed: 21301068]

Jung WH, Yam N, Chen CC, Elawad K, Hu B, Chen Y, 2020. Force-dependent extracellular matrix remodeling by early-stage cancer cells alters diffusion and induces carcinoma-associated fibroblasts. Biomaterials 234. 10.1016/j.biomaterials.2020.119756

Jutz S, Leitner J, Schmetterer K, Doel-Perez I, Majdic O, Grabmeier-Pfistershammer K, Paster W, Huppa JB, Steinberger P, 2016. Assessment of costimulation and coinhibition in a triple parameter T cell reporter line: Simultaneous measurement of NF-κB, NFAT and AP-1. J. Immunol. Methods 10.1016/j.jim.2016.01.007

Kaufman KA, Bowen JA, Tsai AF, Bluestone JA, Hunt JS, Ober C, 1999. The CTLA-4 gene is expressed in placental fibroblasts. Mol. Hum. Reprod 5, 84–87. 10.1093/molehr/5.1.84 [PubMed: 10050667]

Koch TM, Münster S, Bonakdar N, Butler JP, Fabry B, 2012. 3D traction forces in cancer cell invasion. PLoS One 7, e33476. 10.1371/journal.pone.0033476 [PubMed: 22479403]

Kovács M, Tóth J, Hetényi C, Málnási-Csizmadia A, Sellers JR, 2004. Mechanism of Blebbistatin Inhibition of Myosin II. J. Biol. Chem 279, 35557–35563. 10.1074/jbc.M405319200 [PubMed: 15205456]

Kraning-Rush CM, Califano JP, Reinhart-King CA, 2012. Cellular traction stresses increase with increasing metastatic potential. PLoS One 7, e32572. 10.1371/journal.pone.0032572 [PubMed: 22389710]

Laurent S, Queirolo P, Boero S, Salvi S, Piccioli P, Boccardo S, Minghelli S, Morabito A, Fontana V, Pietra G, Carrega P, Ferrari N, Tosetti F, Chang L-J, Mingari M, Ferlazzo G, Poggi A, Pistillo M, 2013. The engagement of CTLA-4 on primary melanoma cell lines induces antibody-dependent cellular cytotoxicity and TNF-α production. J. Transl. Med 11, 108. 10.1186/1479-5876-11-108 [PubMed: 23634660]

Leitner J, Kuschei W, Grabmeier-Pfistershammer K, Woitek R, Kriehuber E, Majdic O, Zlabinger G, Pickl WF, Steinberger P, 2010. T cell stimulator cells, an efficient and versatile cellular system to assess the role of costimulatory ligands in the activation of human T cells. J. Immunol. Methods 10.1016/j.jim.2010.09.020

Li Z, Persson H, Adolfsson K, Abariute L, Borgström MT, Hessman D, Åström K, Oredsson S, Prinz CN, 2017. Cellular traction forces: a useful parameter in cancer research. Nanoscale 9, 19039–19044. 10.1039/C7NR06284B [PubMed: 29188243]

Malinova TS, Huveneers S, 2018. Sensing of Cytoskeletal Forces by Asymmetric Adherens Junctions. Trends Cell Biol. 10.1016/j.tcb.2017.11.002

Mao H, Zhang L, Yang Y, Zuo W, Bi Y, Gao W, Deng B, Sun J, Shao Q, Qu X, 2010. New Insights of CTLA-4 into Its Biological Function in Breast Cancer 728–736.

Meloty-Kapella L, Shergill B, Kuon J, Botvinick E, Weinmaster G, 2012. Notch Ligand Endocytosis Generates Mechanical Pulling Force Dependent on Dynamin, Epsins, and Actin. Dev. Cell 22, 1299–1312. 10.1016/j.devcel.2012.04.005 [PubMed: 22658936]

Nichols JT, Miyamoto A, Weinmaster G, 2007. Notch signaling - Constantly on the move. Traffic. 10.1111/j.1600-0854.2007.00592.x

Northcott JM, Dean IS, Mouw JK, Weaver VM, 2018. Feeling Stress: The Mechanics of Cancer Progression and Aggression. Front. Cell Dev. Biol 6, 17. 10.3389/fcell.2018.00017 [PubMed: 29541636]

Ovcinnikovs V, Ross EM, Petersone L, Edner NM, Heuts F, Ntavli E, Kogimtzis A, Kennedy A, Wang CJ, Bennett CL, Sansom DM, Walker LSK, 2019. CTLA-4-mediated transendocytosis of costimulatory molecules primarily targets migratory dendritic cells. Sci. Immunol 4, eaaw0902. 10.1126/sciimmunol.aaw0902 [PubMed: 31152091]

Park S, Joo YK, Chen Y, 2019. Versatile and High-throughput Force Measurement Platform for Dorsal Cell Mechanics. Sci. Rep 10.1038/s41598-019-49592-1

Park S, Joo YK, Chen Y, 2018. Dynamic adhesion characterization of cancer cells under blood flow-mimetic conditions: effects of cell shape and orientation on drag force. Microfluid. Nanofluidics 22, 108. 10.1007/s10404-018-2132-7

Paulsen E-E, Kilvaer TK, Rakaee M, Richardsen E, Hald SM, Andersen S, Busund L-T, Bremnes RM, Donnem T, 2017. CTLA-4 expression in the non-small cell lung cancer patient tumor microenvironment: diverging prognostic impact in primary tumors and lymph node metastases. Cancer Immunol. Immunother 66, 1449–1461. 10.1007/s00262-017-2039-2 [PubMed: 28707078]

Pico de Coaña Y, Masucci G, Hansson J, Kiessling R, 2014. Myeloid-derived suppressor cells and their role in CTLA-4 blockade therapy. Cancer Immunol. Immunother 63, 977–983. 10.1007/s00262-014-1570-7 [PubMed: 24966003]

Pistillo MP, 2003. CTLA-4 is not restricted to the lymphoid cell lineage and can function as a target molecule for apoptosis induction of leukemic cells. Blood 101, 202–209. 10.1182/blood-2002-06-1668 [PubMed: 12393538]

Pistillo MP, Tazzari PL, Palmisano GL, Pierri I, Bolognesi A, Ferlito F, Capanni P, Polito L, Ratta M, Pileri S, Piccioli M, Basso G, Rissotto L, Conte R, Gobbi M, Stirpe F, Ferrara GB, 2003. CTLA-4 is not restricted to the lymphoid cell lineage and can function as a target molecule for apoptosis induction of leukemic cells. Blood 101, 202–209. 10.1182/blood-2002-06-1668 [PubMed: 12393538]

Przybyla LM, Rubashkin MG, Pickup MW, Tan SJ, Davidson MW, Ye X, Barnes JM, Lammerding J, Ou G, Weaver VM, Chang AC, Lakins JN, Odde DJ, McGregor AL, Bell ES, Cassereau L, DuFort CC, Kai F, Dunn AR, Prahl LS, Mekhdjian AH, 2017. Integrin-mediated traction force enhances paxillin molecular associations and adhesion dynamics that increase the invasiveness of tumor cells into a three-dimensional extracellular matrix. Mol. Biol. Cell 28, 1467–1488. 10.1091/mbc.e16-09-0654 [PubMed: 28381423]

Qureshi OS, Zheng Y, Nakamura K, Attridge K, Manzotti C, Schmidt EM, Baker J, Jeffery LE, Kaur S, Briggs Z, Hou TZ, Futter CE, Anderson G, Walker LSK, Sansom DM, 2011. Trans-Endocytosis of CD80 and CD86: A Molecular Basis for the Cell-Extrinsic Function of CTLA-4. Science (80-.). 332, 600–603. 10.1126/science.1202947

Rudd CE, 2008. The reverse stop-signal model for CTLA4 function. Nat. Rev. Immunol 8, 153–160. 10.1038/nri2253 [PubMed: 18219311]

Sakurai T, Woolls MJ, Jin S-W, Murakami M, Simons M, 2014. Inter-Cellular Exchange of Cellular Components via VE-Cadherin-Dependent Trans-Endocytosis. PLoS One 9, e90736. 10.1371/journal.pone.0090736 [PubMed: 24603875]

Sharma P, Hu-Lieskovan S, Wargo JA, Ribas A, 2017. Primary, Adaptive, and Acquired Resistance to Cancer Immunotherapy. Cell 168, 707–723. 10.1016/j.cell.2017.01.017 [PubMed: 28187290]

Shi D, Guo J, Chen L, Xia C, Yu Z, Ai Y, Li CM, Kang Y, Wang Z, 2015. Differential microfluidic sensor on printed circuit board for biological cells analysis. Electrophoresis. 10.1002/elps.201400524

Shi Y, Porter CL, Crocker JC, Reich DH, 2019. Dissecting fat-tailed fluctuations in the cytoskeleton with active micropost arrays. Proc. Natl. Acad. Sci. U. S. A 10.1073/pnas.1900963116

Sniadecki NJ, Anguelouch A, Yang MT, Lamb CM, Liu Z, Kirschner SB, Liu Y, Reich DH, Chen CS, 2007. Magnetic microposts as an approach to apply forces to living cells. Proc. Natl. Acad. Sci. U. S. A 10.1073/pnas.0611613104

Sniadecki NJ, Lamb CM, Liu Y, Chen CS, Reich DH, 2008. Magnetic microposts for mechanical stimulation of biological cells: Fabrication, characterization, and analysis. Rev. Sci. Instrum 10.1063/1.2906228

Tan JL, Tien J, Pirone DM, Gray DS, Bhadriraju K, Chen CS, 2003. Cells lying on a bed of microneedles: An approach to isolate mechanical force. Proc. Natl. Acad. Sci 100, 1484–1489. 10.1073/pnas.0235407100 [PubMed: 12552122]

Thompson CB, Allison JP, 1997. The emerging role of CTLA-4 as an immune attenuator. Immunity. 10.1016/S1074-7613(00)80366-0

Tsoukas CD, Landgraf B, Bentin J, Valentine M, Lotz M, Vaughan JH, Carson DA, 1985. Activation of resting T lymphocytes by anti-CD3 (T3) antibodies in the absence of monocytes. J. Immunol 135, 1719–23. [PubMed: 3926881]

Vijayakrishnan L, Slavik JM, Illés Z, Greenwald RJ, Rainbow D, Greve B, Peterson LB, Hafler DA, Freeman GJ, Sharpe AH, Wicker LS, Kuchroo VK, 2004. An autoimmune disease-associated CTLA-4 splice variant lacking the B7 binding domain signals negatively in T cells. Immunity 20, 563–575. 10.1016/S1074-7613(04)00110-4 [PubMed: 15142525]

Walker LSK, 2017. PD-1 and CTLA-4: Two checkpoints, one pathway? Sci. Immunol 2, eaan3864. 10.1126/sciimmunol.aan3864 [PubMed: 28529997]

Walker LSK, Sansom DM, 2011. The emerging role of CTLA4 as a cell-extrinsic regulator of T cell responses. Nat. Rev. Immunol 11, 852–863. 10.1038/nri3108 [PubMed: 22116087]

Wang X, Ha T, 2013. Defining Single Molecular Forces Required to Activate Integrin and Notch Signaling. Science (80-.). 340, 991–994. 10.1126/science.1231041

Wang X, Rahil Z, Li ITS, Chowdhury F, Leckband DE, Chemla YR, Ha T, 2016. Constructing modular and universal single molecule tension sensor using protein G to study mechano-sensitive receptors. Sci. Rep 6, 21584. 10.1038/srep21584 [PubMed: 26875524]

Wing K, Yamaguchi T, Sakaguchi S, 2011. Cell-autonomous and -non-autonomous roles of CTLA-4 in immune regulation. Trends Immunol. 10.1016/j.it.2011.06.002

Xue P, Zhang L, Guo J, Xu Z, Kang Y, 2016. Isolation and retrieval of circulating tumor cells on a microchip with double parallel layers of herringbone structure. Microfluid. Nanofluidics 10.1007/s10404-016-1834-y

Yu H, Yang J, Jiao S, Li Y, Zhang W, Wang J, 2015a. Cytotoxic T lymphocyte antigen 4 expression in human breast cancer: implications for prognosis. Cancer Immunol. Immunother 64, 853–60. [PubMed: 25893809]

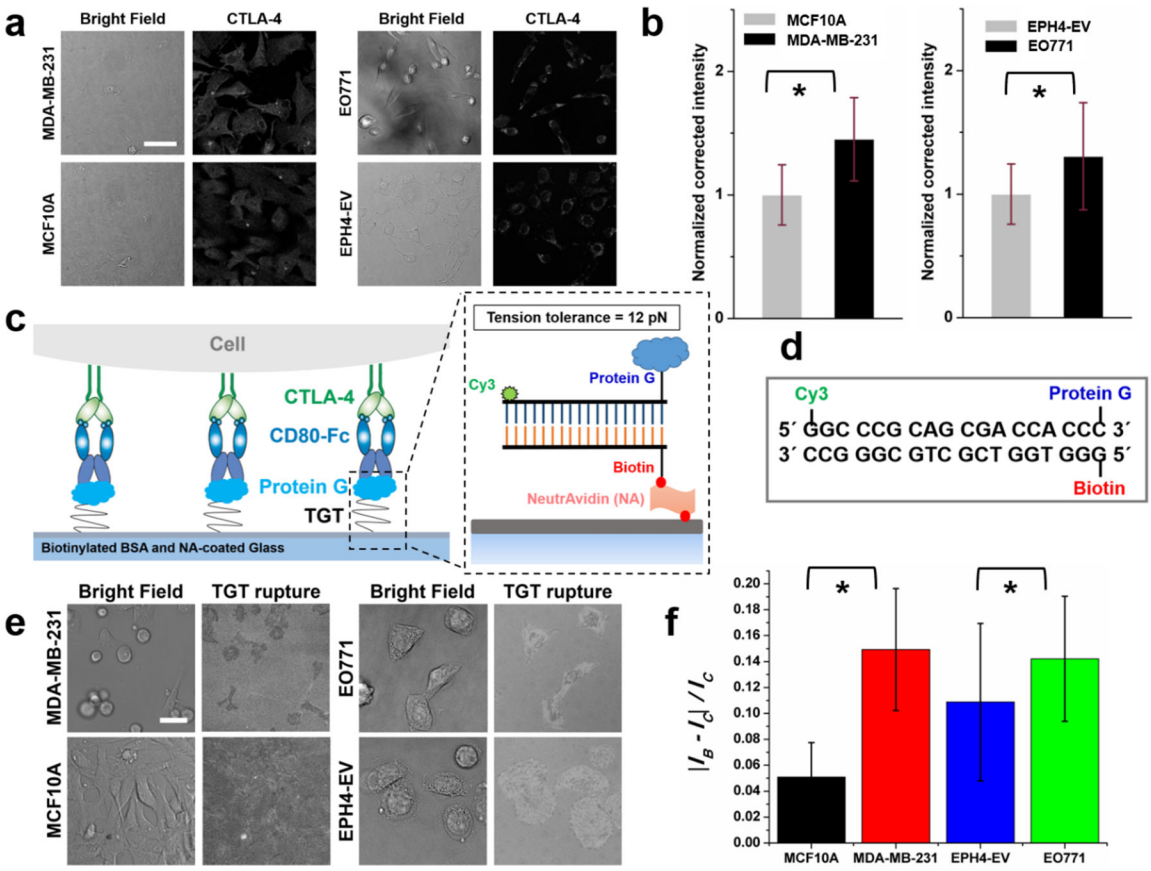

Figure 1:

The bond between CD80 and CTLA-4 on cancer cells experiences higher tension than on normal cells. **a**. CTLA-4 can be detected by immunofluorescence in normal mammary gland epithelial cells (MCF10A and EpH4-EV) and cancer cells (MDA-MB-231 and EO771). Scale bar: 50 μm. **b**. Image analysis of the immunofluorescence showed that the expression level of CLTA-4 was relatively higher by approximately 30% to 40% in the cancer cells (n=81, 72, 69, 53 for MCF10A, EpH4-EV, MDA-MB-231 and EO771 cells respectively). **c**. The diagram illustrates that a tension gauge tether (TGT) can be used to determine whether forces transmitted through CTLA-4 by cells exceed 12 pN at the single-molecule level. If yes, the DNA strand conjugated with Cy3 will be torn apart from the DNA strand immobilized on the glass substrate, an event termed “rupture”, resulting in loss of fluorescent signals. **d**. The DNA sequence encoded for the TGT and the molecules conjugated to the DNA are illustrated. **e**. TGT ruptures were recorded against the bright background. Scale bar: 20 μm. **f**. Image analysis showed that 1.3 to 2.9-fold higher rupture events were recorded in cancer cells relative to normal cells (n=7, 8, 5, 8 for MCF10A, EpH4-EV, MDA-MB-231 and EO771 cells, respectively). I_B and I_C indicate the average background intensity and average intensity in the cell. *p<0.05

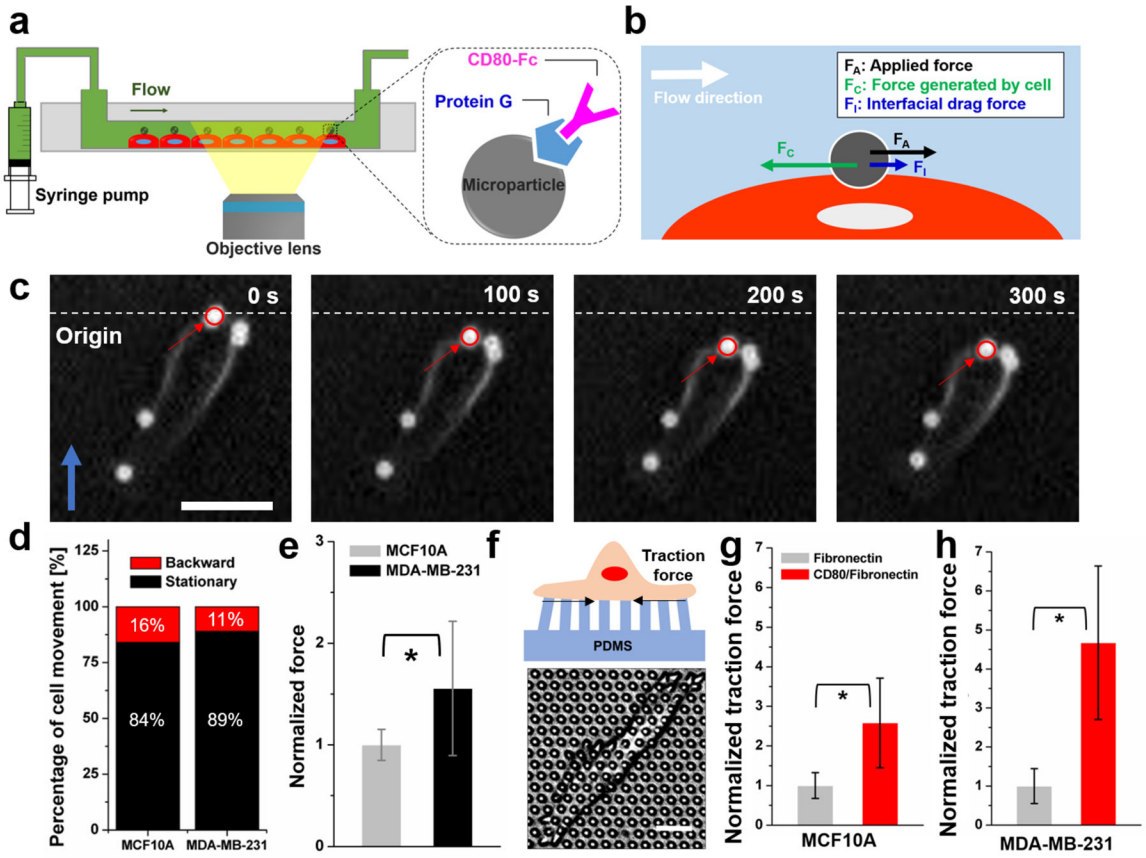

Figure 2:

Higher traction forces transmitted via the bond between CTLA-4 and CD80 are detected in both the ventral and dorsal sides of cancer cells. **a**. Schematic drawing illustrating how dorsal traction force measurement is performed in a flow chamber. 2.8-μm particles conjugated with CD80 are bound to the cells and subsequently tracked to estimate the force generated by the cells against the flow direction. **b**. The magnitude of the dorsal traction force generated by the cell (F_C) is the vector sum of the applied force (F_A) provided by the flow and the interfacial drag force (F_I). **c**. A representative time-lapse image series is shown to visualize the displacement of particles bound to a cancer cell (MDA-MB-231) against the flow, the direction of which is indicated by the blue arrow. The dashed line marks the horizontal position at 0 sec. Scale bar: 20 μm. **d**. 16% of the cell-bound particles in MCF10A cells and 11% in MDA-MB-231 cells were detected to move against the flow direction and were analyzed to estimate the dorsal traction forces (n=91 and n=111 for MCF10A and MDA-MB-231 cells, respectively). **e**. The dorsal traction forces generated by MDA-MB-231 cells were approximately 50% higher than the values measured in MCF10A cells (n=10). **f**. Schematic drawing illustrating how forces transmitted via the bond between CTLA-4 and CD80 at the ventral side of the cell can be measured using arrays of compliant micropillars coated with CD80 and fibronectin. A representative image of a MDA-MB-231 cell exerting forces to bend the micropillars. Scale bar: 10 μm. **g-h**. The ventral forces on CD80/fibronectin-coated micropillars were 2.58 and 4.67 times higher than the values

measured on fibronectin-coated micropillars for MCF10A and MDA-MB-231, respectively (n = 9). *p<0.05

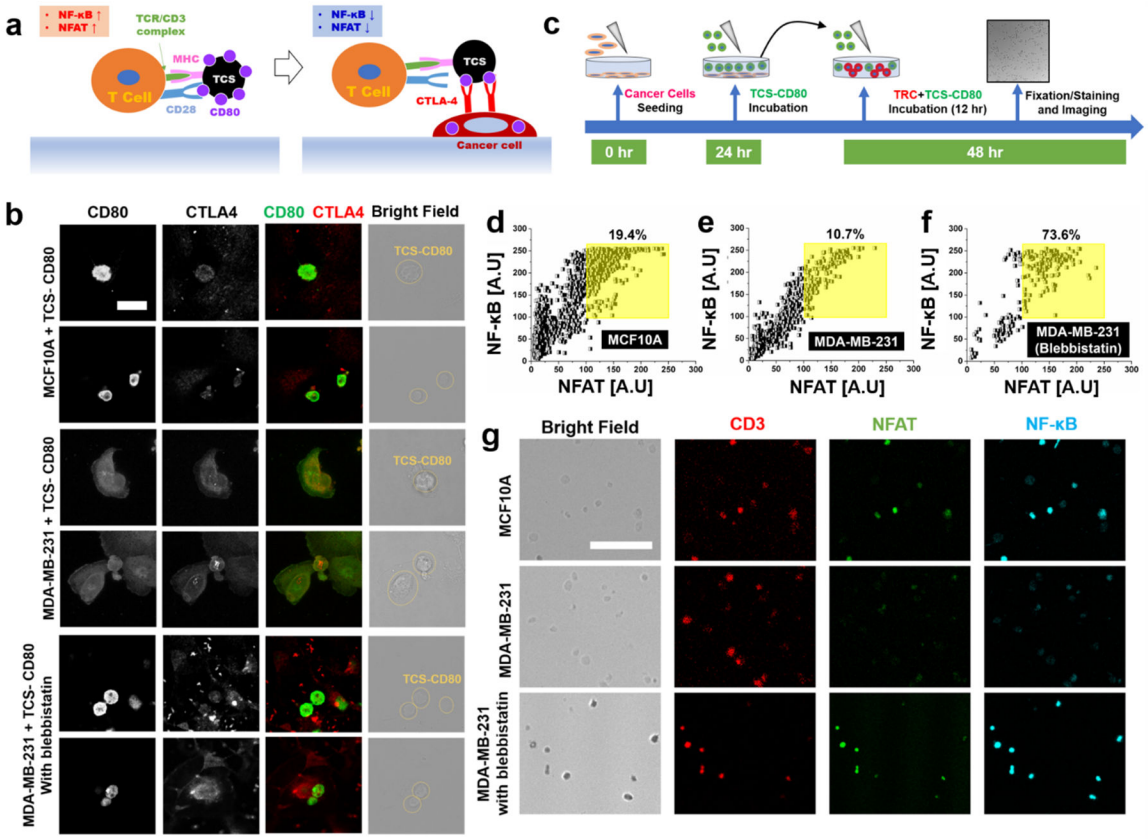

Figure 3:

Force-dependent trans-endocytosis of CD80 by cancer cells reduces the T cell-activation capacity in TCS-CD80 cells. **a**. The schematic drawing illustrates that TCS-CD80 cells, and Jurkat T cells expressing both NF-κB-CFP and NFAT-eGFP (TRCs) are used to assess whether cancer cells deplete CD80 on TCS-CD80 cells and subsequently suppress their capacity to activate T cells. **b**. Immunofluorescence showed that CD80 was trans-endocytosed, and thus depleted on the surface of TCS-CD80 cells when co-incubated with MDA-MB-231 cells. Inhibition of myosin activity in MDA-MB-231 cells by blebbistatin suppresses the trans-endocytosis. Note CTLA-4 was enriched at the interface where TCS-CD80 cells were bound to MDA-MB-231 or MCF10A cells. Scale bar: 20 μm. **c**. The schematic drawing illustrates the steps of the T cell activation assay. TCS-CD80 cells were co-incubated with cancer cells (MDA-MB-231) for 12 hours, and then transferred to be co-incubated with TRCs for 4 hours. TRCs, identified by the positive anti-CD3 staining, were then imaged to evaluate whether NF-κB- and NFAT- mediated transcription of CFP and eGFP is elevated. **d-f**. Image analysis of CFP and eGFP intensity, driven by NF-κB and NFAT activities, respectively, showed that the T cell activation was 50% less effective by TCS-CD80 cells co-incubated with MDA-MB-231 cells (n=1306), compared to the ones with MCF10A cells (n=1983). Inhibition of myosin activity in MDA-MB-231 cells by blebbistatin increased the T cell activation capacity of TCS-CD80 by ~ 7-fold (n = 220). **g**. NF-κB (cyan)- and NFAT (green)-dependent gene expression was assessed in TRCs (red) co-incubated with TCS-CD80 cells previously in contact with MCF10A, MDA-MB-231, and myosin-inhibited MDA-MB-231 cells. Scale bar: 100 μm.

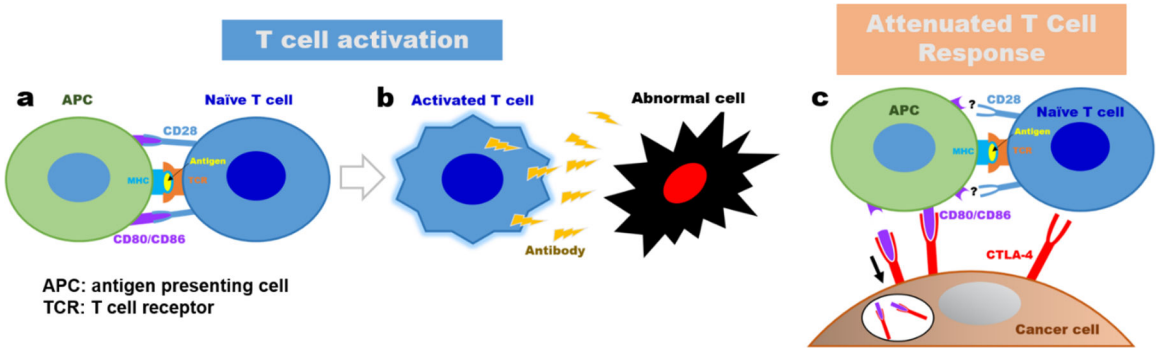

Figure 4:

The schematic depiction of the working model regarding attenuated T cell activation by force-dependent depletion of CD80 on APCs. **a**. Normally APCs activate Naïve T cells with the involvement of CD80. **b**. The activated T cell targets abnormal cells and initiates programmed cell death. **c**. CD80 on the surface of APCs might be depleted by force-dependent trans-endocytosis, resulting in attenuation of T cell response to cancer cells.